POAC 2019
DELFT THE NETHERLANDS

Proceedings of the 25th International Conference on
Port and Ocean Engineering under Arctic Conditions
June 9-13, 2019, Delft, The Netherlands

Physical experiments of internal solitary waves (ISWs) under various ice conditions in a cold laboratory

Karl-Ulrich Evers[1], Andrea Haase[2], Magda Carr[3]
[1] Solutions4Arctic, Hamburg, Germany
[2] Hamburg Ship Model Basin, Hamburg, Germany
[3] School of Mathematics, Statistics and Physics - Newcastle University, Newcastle, UK

ABSTRACT

Internal solitary waves (ISWs) propagate along density interfaces in a two layer fluid. A better understanding of ISW dynamics in the Arctic Ocean and, in particular, how the ISW field is affected by changes in both ice cover and stratification, is central in understanding how the rapidly changing Arctic will adapt to climate change. Experiments are conducted in a cold laboratory at the Hamburg Ship Model Basin (HSVA). The aim of the experimental campaign is to generate internal solitary waves (ISWs) in a stratification in which the upper boundary varied from open water to different ice types, including, nilas ice, grease ice and level ice. For this study a customized flume is designed and built. Specific objectives are to generate ISWs and to obtain accurate measurements of (i) wave amplitude, (ii) wave-induced velocity field, and (iii) wave speed under the varying ice conditions. In addition, measurements of ice thickness and wave-induced floe speed are made. The main questions to address are (i) what is the dissipation of ISW energy under different ice conditions- and (ii) what is the effect of ISW energy on the ice dynamics?

KEY WORDS: Ice; ISW; Experiments in ice flume; Stratification; Ice dynamics

INTRODUCTION

Oceanic internal solitary waves (ISWs) propagate along density interfaces and are ubiquitous in stratified water. Their properties are influenced strongly by the nature and form of the upper and lower bounding surfaces of the containing basin(s) in which they propagate. As the Arctic Ocean evolves to a seasonally more ice-free state, the ISW field will be affected by the change. The relationship between ISW dynamics and ice is crucial in understanding (i) the general circulation and thermodynamics in the Arctic Ocean and (ii) local mixing processes that supply heat and nutrients from depth into upper layers, especially the photic zone. This, in turn, has important ramifications for sea ice formation processes and the state

of local and regional ecosystems.

It is known that ISWs cause flexure of sea ice (Czipott *et al*., 1991; Marchenko et al., 2010) and theoretical studies suggest that they are responsible for the formation of ice bands in the marginal ice zone (MIZ).

The effect of diminishing sea ice cover on the ISW field is not well established to date. A better understanding of ISW dynamics in the Arctic Ocean and, in particular, how the ISW field is affected by changes in both ice cover and stratification, is central in understanding how the rapidly changing Arctic will adapt to climate change.

There is a clear need to supplement field work with modelling studies. Experiments are executed in the Arctic Environmental Test Basin (AETB) at the Hamburg Ship Model Basin (HSVA) as part of the *Hydralab+ Transnational Access* project (www.hydralab.eu). Researchers from France, Germany, Norway and the United Kingdom are involved in the experiments where laboratory investigation of ISWs in a two-layer stratified flow propagating from open water to under different ice features is carried out. This is the first time that ISWs have been generated under ice in a laboratory. The objective of this study is to generate ISWs under different ice types, namely, nilas, grease, and level ice. The main focus of the experiments was to (i) obtain accurate measurements of the wave induced velocity field under the ice and (ii) get a qualitative understanding of how different ice conditions affect the ISW field.

This study presents the test set-up, model ice production and test performance. The data processing and data analysis is still ongoing and detailed results will be published in *Geophysical Research Letters* (Carr *et al.*, 2019).

EXPERIMENTAL SET-UP AND PROCEDURE

General description

The experiments are carried out in the cold room Arctic Environmental Test Basin (AETB). In the cold room AETB there is a basin of 30m length, 6m width and 1.5m depth and has a volume of 270m^3. The room can be cooled down to a temperature of -15°C. For the experiments the basin was emptied and a flume was designed and custom-built. The flume has the dimension of 6m in length, 0.5m in width and 0.6m in depth and consists of rectangular aluminium profiles (type Bosch-Rexroth 45/45; 90/90 and 90/180mm) with corner connections and 15 mm thick transparent Plexiglass® plates (*Fig. 1*). The Flume is composed of 2 Plexiglass® elements (length=3000m, width=470mm and height=600mm) which has a total length of 6000mm and is based on a foundation that also consists of rectangular aluminium profiles (12 supports). The Plexiglass® construction allows visualisation from the side and illumination from below. The total height of the experimental set-up is about 1.7m.

The flume is filled with homogeneous salt water of prescribed density ρ_3 = 1045 kg/m^3 to a depth h_3. Less dense brine solution of density ρ_1 = 1025 kg/m^3 is then slowly added to the top of the dense salt water layer via an array of floating sponges (*Fig. 2*). Consequently, an interface (pycnocline) between the two fluids forms in which the density, varies as a linear function of depth z. After the flume is stratified ice will then be made at the surface, such that half the surface is ice-covered and the other half is ice-free. *Figure 3* shows a schematic diagram of the flume arrangement.

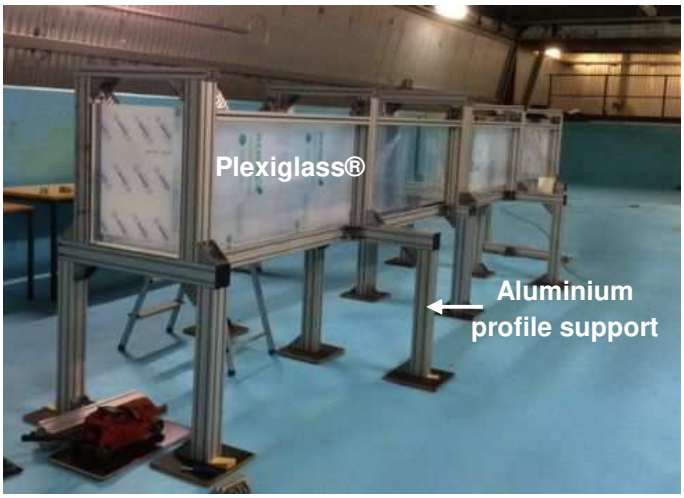

Figure 1. Plexiglass® flume (6m x 0.47m x 0.6m) installed in HSVA's Arctic Environmental Test Basin (AETB)

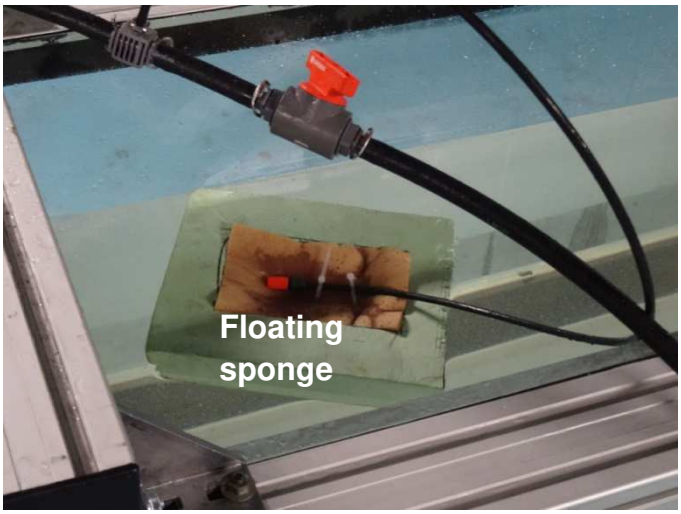

Figure 2. Brine solution of density $\rho_l = 1025$ kg/m^3 is added via an array of floating surface sponges

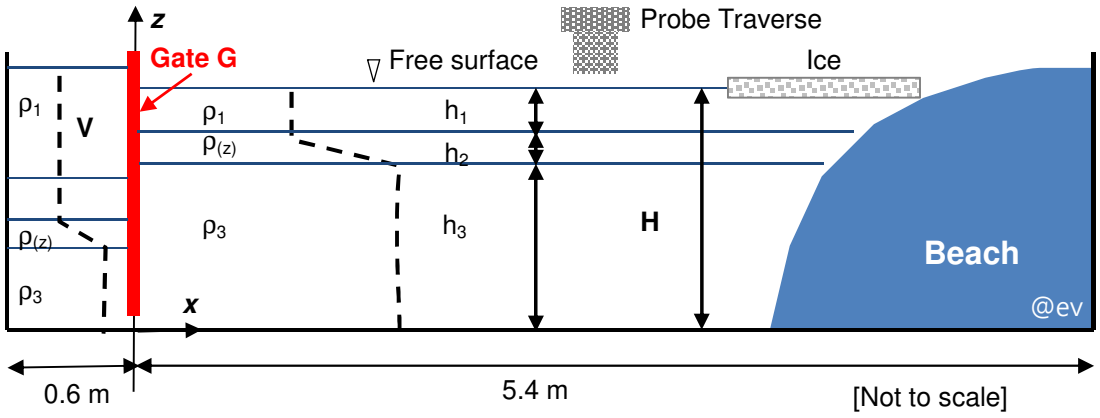

Figure 3. Schematic diagram of the flume arrangement

Production of ice

Different types of ice are frozen on the surface or produced in the Large Ice Model Basin (LIMB) and added on the surface in the flume.

(i) **Level ice** is made in HSVA's Large Ice Model Basin (LIMB). HSVA's current model level ice is frozen from a 0.7% sodium chloride solution in the natural way, i.e. the water/ice surface is exposed to cooled air. The preparation of the ice sheet is started by a seeding procedure. For this purpose water is sprayed into the cold air of the ice tank. The droplets freeze in the air forming small ice crystals which settle on the water surface. By this method the growth of a fine-grained ice of primarily columnar crystal structure is initiated. Tank water which has been pressure-saturated with air is uniformly discharged along the tank bottom during the entire freezing process. Immediately after discharging, the surplus air segregates from the water and forms tiny air bubbles. These air bubbles whose diameter range from 200−500 microns rise to the ice sheet, where they are embedded into the growing ice crystals. Another advantage of the air content in the ice is the possibility to adjust the ice density so that the density difference between ice and water is within the natural range. Finally the embedded air bubbles give the model ice a white appearance (Evers & Jochmann, 1993; Evers, 2015). When the ice sheet reaches a certain thickness sections are cut and removed from the LIMB, and then kept in a cold storage unit on boards of wood until required. The floes of level ice, sitting on wood, are carefully lowered into the stratification and then the wood slid out from beneath them (*Fig. 4*).

(ii) **Grease ice/slush and brash ice** is made in buckets by crushing model level ice. The grease ice is then carefully added to the surface of the water column using a grate and hand shovel (*Fig. 5*). The grate is placed in the top layer of the water column, care is taken not to disturb the pycnocline and the grease ice is slowly poured over the grate using the hand shovel. The grate is then removed from the water column.

(iii) **Nilas ice** is made by reducing the temperature in the AETB so that the surface of the water column freezes (*Fig. 6*). Open water sections are maintained by placing styrofoam at the surface during the freezing process. The styrofoam lids are removed just prior to an experiment commencing.

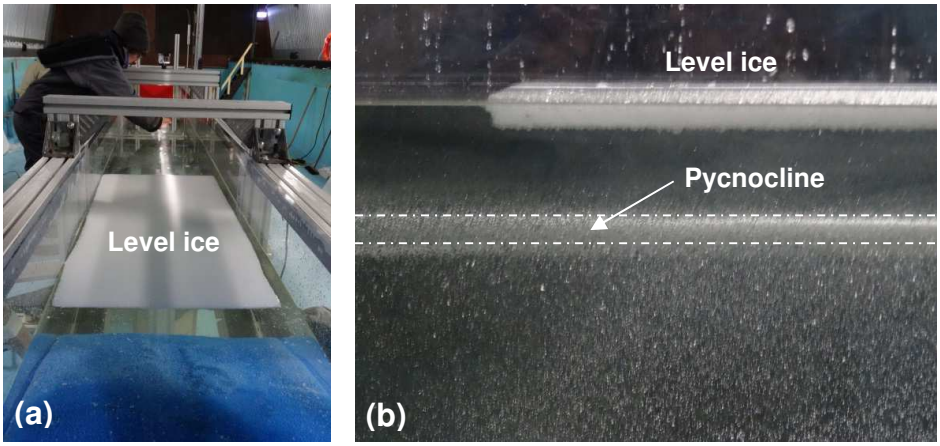

Figure 4. Level ice plate in the stratified flume (a and b); the pycnocline is shown in (b)

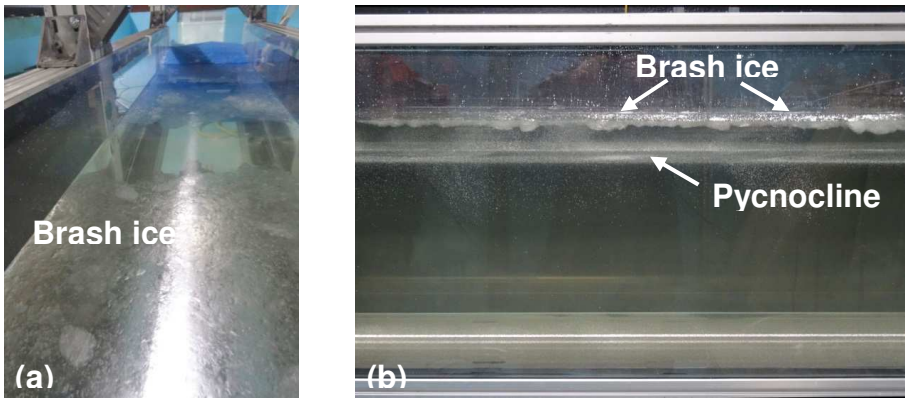

Figure 5. Brash ice is used in the stratified flume (a and b); the pycnocline is shown in (b)

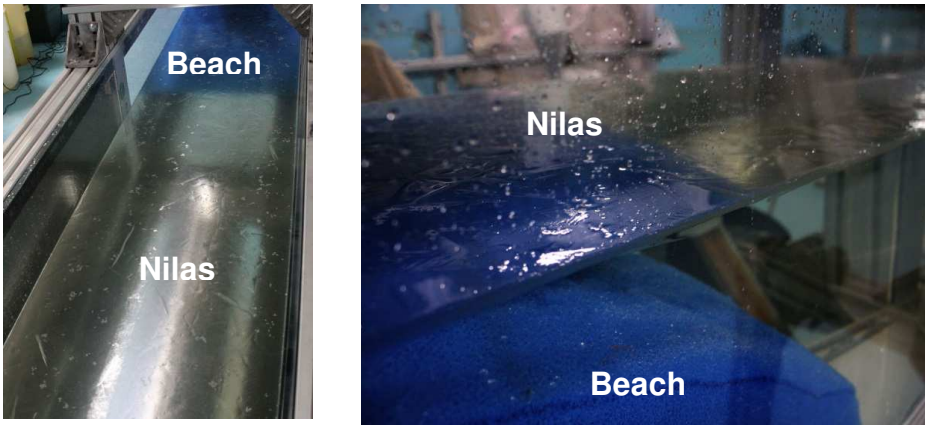

Figure 6. Nilas is frozen in the stratified flume

A gate is inserted at the upstream end of the flume (*Fig. 7a*) and lowered approximately 1 cm above the bottom of the flume.

A beach consisting of polyether filter foam (*Fig. 7b*) is placed at the downstream end of the flume and absorbs some of the ISW energy. A fixed Volume V, of water density ρ_1 is then added behind the gate. Due to hydrostatic balance, fluid density ρ_3 flows under the gate into the main section of the flume. After the Volume, V, is added, the entire fluid depth H, in the main section of the flume is measured using a pre-set tape on the Plexiglass® window. During filling the air temperature is kept just above T= 0°C.

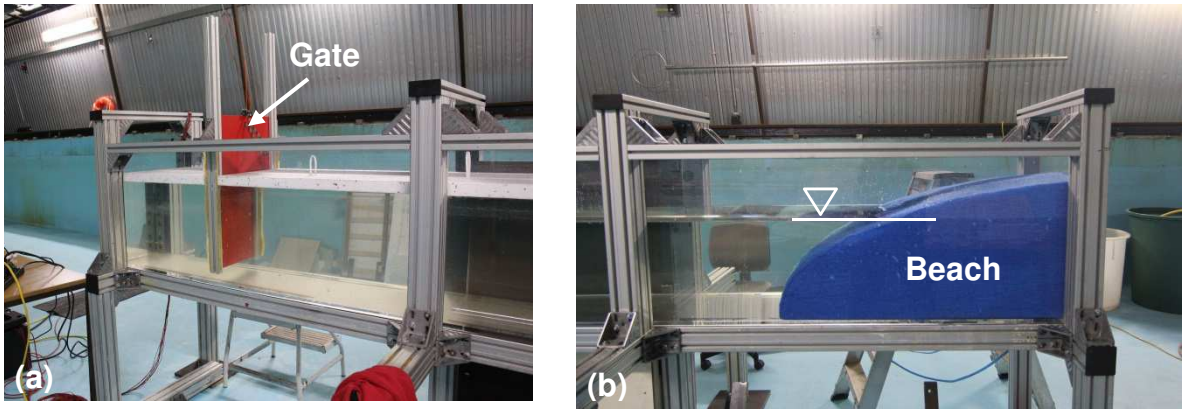

Figure 7. Arrangement of gate (a) and beach (b) in the flume

Instrumentation and data acquisition

Stratification of the fluid is measured by means of MSCTI high precision micro-conductivity sensors (Precision Measurement Engineering). Micro-conductivity readings are taken just prior to an experiment commencing. The micro-conductivity probes sampled at 10 kHz.

Three UNIQ UP-1830CL-12B 2/3" 1024 x 1024 Mono 12 bit digital cameras attached to R64-PCE-CL-D R64e PCI Express frame grabbers are used to record the fluid motion. The cameras are set up outside of the flume and views the flow field orthogonally from the side. Video capture takes place throughout an experiment. The cameras are arranged so that they have overlapping fields of view and a light source is used such that the cameras can be synchronised in time (*Fig. 8a*). The *UNIQ* cameras sample at 30 frames a second.

A *GoPro Hero 4* camera is set up above the flume (upstream) and views the surface of the water column from above and the *MSCTI* sensor (*Fig. 8b*).

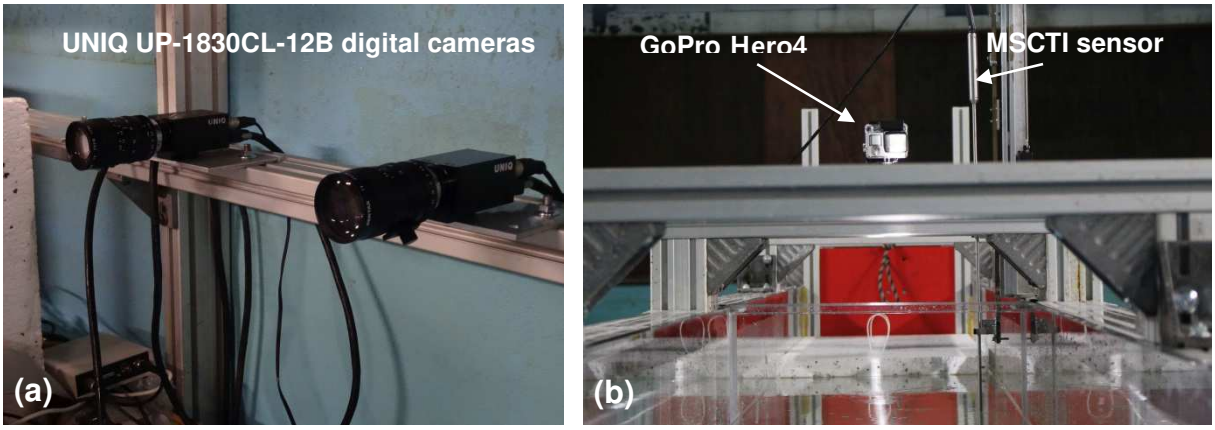

Figure 8. The photo shows 2 of 3 used UNIQ cameras (a); position of *GoPro Hero 4* camera and *MSCTI* conductivity sensor

For the determination of ice thickness calipers are used. To measure the temperature and the salinity of the water in the reservoirs before and during the experiment a measurement device of Type *WTW Multi 3310 IDS* equipped with a conductivity cell of type *WTW TetraCon 925* is used. To measure ice core temperature a thermometer of type *Testo 720* is used. To measure the density of the water used for stratification a generic areometer is used.

The room temperature at different locations of the AETB is recorded continuously during the campaign. The water temperature in the flume is recorded continuously during the campaign by means of a *PT100* sensor chain. A photo of the sensor arrangement is given in *Figure 9.*

Channel	Height above base of flume [mm]
Ch 1	550 (air)
Ch 2	500 (air)
Ch 3	425 (air, sometimes water)
Ch 4	375 (water usually top layer)
Ch 5	275 (water usually bottom layer)
Ch 6	175 (water bottom layer)
Ch 7	100 (water bottom layer)
Ch 8	50 (water bottom layer)

Figure 9. *PT 100* sensor arrangement

Digital cameras with video function (*Canon EOS 600D* and *SONY Cybershot DSC-HX50V*) are used for the documentation of test procedures.

Determination of ice properties

The flexural strength of the ice was determined by two different methods. The in situ measurement in the flume is carried out on cantilevers with a *Chatillon* gauge (*Fig. 10*) and in the other procedure the 3-point-loading method is used (*Fig. 11*). The results of the cantilever beam tests are summarized in *Table 1* and the results of the 3-point-loading tests in *Table 2* respectively.

(i) In situ cantilever beam tests

The flexural ice strength of cantilevers beams is calculated:

$$\sigma_f = \frac{6FL}{BH^2} \tag{1}$$

where

F is the Force [N]
L is the breaking length [mm]
B is the beam width [mm]
H is the ice thickness [mm]

Table 1. Summary of cantilever beam test results (Test date: 18-04-2018 Chatillon gauge)

Run	Force F	Length L	Breadth B	Thickness H	Strength σ
[-]	[N]	[mm]	[mm]	[mm]	[kPa]
1	5.50	96	28	13	669
2	n.a.	n.a.	n.a.	n.a.	n.a.
3	5.27	95	28	12	745
4	5.10	95	30	13	573
5	3.90	94	29	12.5	485
6	4.05	106	29	12.5	568

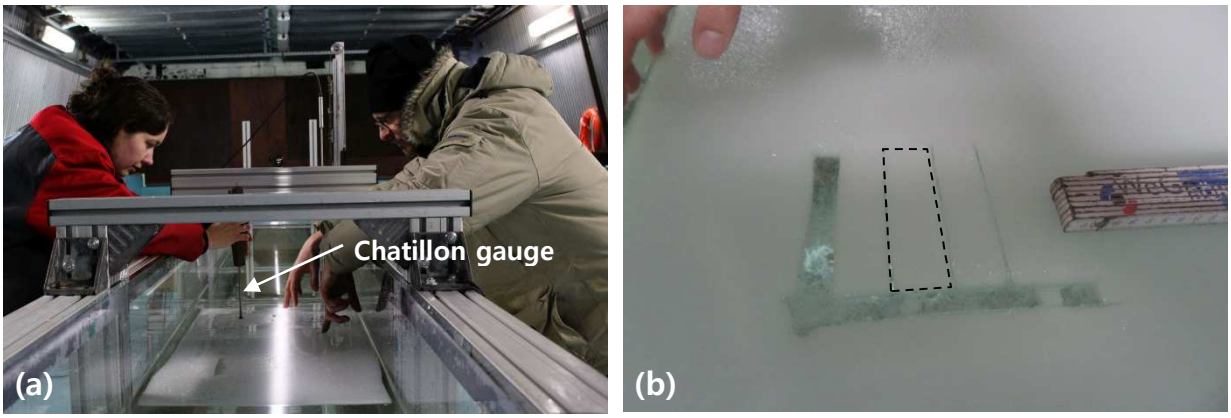

Figure 10. Chatillon gauge used for in situ strength measurement (a), ice beams cut in the level ice sheet (b)

3-Point-Loading Tests

The flexural ice strength is calculated:

$$\sigma_f = 1.5 \frac{FL_0}{BH^2} \qquad (2)$$

where

F is the Force [N]
B is the beam width [mm]
H is the ice thickness [mm]
L_0 is the distance between supports) [mm]

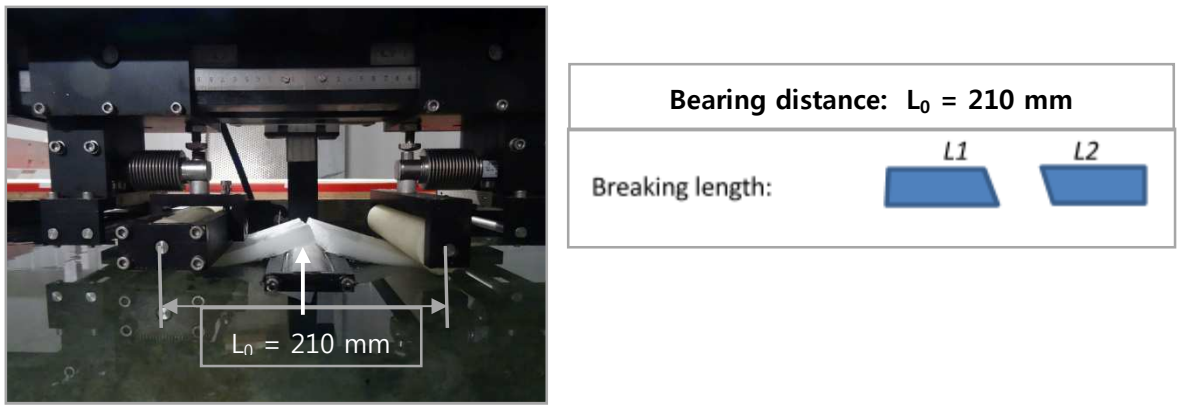

Figure 11. The 3-point-loading device, the ice beam is arranged below the supports. The distance between supports is L_0 = 210mm. A piston moves upwards at constant speed and the beam fails.

Table 2. Summary of 3-point-loading test results (Test date: 18-04-2018)

Sample No.	Force F [N]	Length L [mm]	Breadth B [mm]	Thickness H [mm]	Strength σ_f [kPa]	Breaking Length L_1 [mm]	Breaking Length L_2 [mm]
1*)	53.5	300	100	15	749	160/170	140/130
2*)	57.0	300	98	13	1084	155/170	145/130
3*)	46.0	300	100	13	857	155/170	145/130
4**)	35.0	300	100	12	766	165	135
5**)	41.0	270	100	12	897	145/155	125/115

*) ice sampled from 1st flume experiment;
**) ice sampled from 2nd flume experiment

(ii) Ice density

Ice was sampled from the flume and the ice density was determined. The results from test day 18-04-2018 are summarized in *Table 3*.

Table 3. Results of ice density measurements

Run [-]	Length L [m]	Breadth B [m]	Thickness H [m]	Weight G [kg]	Volume V $1*10^{-04}$ [m3]	Density ρ_{ice} [kg/m3]
1	0.098	0.089	0.014	0.980	1.22108	803
2	0.098	0.100	0.015	0.115	1.47000	782

PERFORMANCE OF EXPERIMENTS

Test program

The table below provides a summary of the experimental runs. “Date” is the date of the experiment, “Run” is the run number for a given day, “Ice type” provides a summary of the ice type, “h3”, “h2”, “h1” are the stratification layer thicknesses. H is the total fluid depth and V is the wave generating volume of fluid added behind the gate.

Table 4. Experiment programme

Date	Run	Ice type	h_3	h_2	h_1	H	V
[ddmmyyyy]	[-]	[-]	[mm]	[mm]	[mm]	[mm]	[$1*10^6$ mm^3]
10-04-2018	1	Nilas smooth & thin -	322	35	43	399	31
	2	Nilas thick & rough -	307	37	68	412	31
	3	Grease - whole surface	276	57	90	424	31
12-04-2018	1	Grease - surface	323	31	44	399	31
	2	Grease - surface	330	35	55	420	60
17-04-2018	1	Nilas - surface partially covered but fixed in x	321	35	44	400	31
	2		332	30	57	420	60
18-04-2018	1	Thin level ice - surface partially covered, free to move	316	38	47	401	30
	2		323	42	55	421	60
19-04-2018	1	Thick level ice - surface partially covered, free to move	302	60	45	406	31
	2		314	59	53	426	61
	3	Thick level ice and double length	313	56	83	452	60

*) “h3”, “h2”, “h1” are the stratification layer thicknesses, H is the total fluid depth and V is the wave generating volume of fluid added behind the gate.

Wave generation

ISWs are generated by removal of the gate which is lifted quickly and smoothly in the vertical direction. After a distance of about 1 m, an ISW of depression propagates along the pycnocline into the main section of the flume. Once an experiment is finished and the water column is stationary, the gate, is reinserted and a fixed volume of fluid of density ρ_1 is again added behind the gate. The micro-conductivity sensors are used again to measure the form of the new stratification before a second (and sometimes third) wave are generated and measured.

When the test is finished, the water may calm down before the gate is reused and the next test run is prepared. The gate is re-inserted and a fixed volume of fluid with density ρ_1 is added behind the gate and the next experiment can start.

Measurement and visualisation of flow

Micro-conductivity sensors are moved vertically through the water column in order to obtain density profiles. The analysis is restricted to two dimensions (x, z) where x denotes the horizontal and z the vertical direction. The different layers of the stratification is denoted by h_1, h_2 and h_3 respectively.

In order to make the streamlines of the flow visible the water column is seeded with boyancy-free, light-reflecting tracer particles of "Pliolite" having grains in the range 150 – 300 microns. These tracer particles are added before the ice is placed in the flume and later under the ice using a thin tube.

Beneath the transparent base of the flume a light source (intensive LED strip passing through a double slit) is placed. This generates a thin vertical column of light illuminating a 2D-slice of the flow field in the mid-plane of the flume.

Three fixed digital video cameras (*UNIQ UP-1830CL-12B*) are set up outside the flume in a fix position. The cameras are synchronized in time and two are positioned to have overlapping fields of view. The video records are processed by software package *DigiFlow*. From time series function of *DigiFlow* the wave speed c, wave amplitude a, wave length λ and wave- induced ice floe speed c_f.

The PIV-function of *DigiFlow* is used to calculate continuous synoptic velocity and vorticity field data along the illuminated cross-section in the middle part of the flume.

SUMMARY AND CONCLUSIONS

The objective of this study is to generate ISWs under different ice types, namely, nilas, grease, and level ice. The main focus of the experiments is to (i) obtain accurate measurements of the wave induced velocity field under the ice and (ii) get a qualitative understanding of how different ice conditions affect the ISW field.

ISWs are generated using a sluice gate and the surface condition is varied from (i) nilas or grease ice covering the full length of the tank, to (ii) grease or level ice with an edge such that the surface condition changed from open water to ice cover with the ice cover being free to move. Measurements of wave speed, wave amplitude and wave induced velocity under the ice are obtained in the mid-plane of the tank. Difficulties in visualisation very close to the bottom side of the ice are encountered due to (i) reflection of the light source off the underside of the ice and (ii) ice at the front of the tank obstructing the field of view.

The experiments showed that the internal wave-induced flow at the surface is capable of transporting ice floes in the horizontal direction at a speed comparable to the wave speed. It

is anticipated that the results will allow the transport speed of the ice to be parameterised in terms of the wave induced horizontal velocity, the wave length, the floe thickness, the floe ice type and the floe length respectively.

In thick ice cover cases, in which the thickness of the ice was comparable to the depth of the top layer in the stratification, the ice significantly damped the ISW signal causing the wave to break and even be destroyed in some cases.

The roughness associated with different ice types caused varying degrees of vorticity and turbulence in the wave-induced boundary layer beneath the ice. It is hoped that the velocity data obtained (via PIV) can be used to analyse wave dissipation rates for different wave properties and ice types.

The range of investigated parameters was limited by the duration of the experimental campaign and the scale of the flume. The experiments are original and unprecedented; combining stratified ISW flow with ice.

Preliminary results and observations indicate the need for further more detailed investigations and show clearly that the physical interactions of ISWs with ice have significant implications for wave energy dissipation and mixing processes in polar oceans.

ACKNOWLEDGEMENT

The work described in this publication was supported by the European Community's Horizon 2020 Research and Innovation Programme through the grant to HYDRALAB-PLUS, Contract no. 654110. This work received funding from the MASTS pooling initiative (The Marine Alliance for Science and Technology for Scotland) and their support is gratefully acknowledged. The authors thank Gesa Ziemer and Nis Schnoor from HSVA for providing technical assistance during the experiments.

REFERENCES

Carr, M., Haase, A., Evers, K.-U., Fer, I., Thiem, Ø., Berntsen, J., Părău, E. Kalisch, H., Sutherland, P., and Davies, P. A. (2019). Laboratory Experiments on Internal Solitary Waves in Ice-Covered Waters. *Submitted to American Geophysical Union (AGU) - Geophysical Research Letters*

Czipott, P.V., Levine, M.D., Paulson, C.A, Menemenlis; D., Farmer, D.M, & Williams, R.G. (1991). Ice flexure forced by internal wave packets in the Arctic Ocean. *Science*, 254, 832-835.

Evers, K.-U. (2015). Modeling ice processes in laboratories and determination of model ice properties. In P. Langhorne (Ed.), Cold regions science and marine technology. EOLSS Publishers

Evers & Jochmann (1993) An Advanced Technique to Improve the Mechanical Properties of Model Ice Developed at the HSVA Ice Tank. *Proceedings 12th POAC'93 Conference*, Hamburg, Germany, August 17-20, 1993.

Marchenko, A.V., Morozov, E., Muzylev, S.V., & Shestov, A.S. (2010). Interaction of short internal waves with ice cover in an Arctic fjord. *Oceanology, 50,* 18-27